Ice and snow cover of continental water bodies from simultaneous radar altimetry and radiometry observations.

Paper for the thematic issue of Survey in Geophysics on "Hydrology from space"

A. V. Kouraev[1,2], M.N. Shimaraev[3], P.I. Buharizin4, M.A. Naumenko[5]
J-F. Crétaux[1], N. Mognard[1], B. Legrésy[1], F. Rémy[1]

1) Laboratoire d'Etudes en Géophysique et Océanographie Spatiales (LEGOS), Toulouse, France
2) State Oceanography Institute, St. Petersburg branch, Russia
3) Limnological Institute, Siberian Branch of Russian Academy of Sciences, Irkutsk, Russia
4) Astrakhan expedition base of the Water Problems Institute of Russian Academy of Sciences, Dept. of Engineering Ecology, Astrakhan, Russia;
5) Institute of Limnology of Russian Academy of Sciences, ST. Petersburg, Russia

Abstract

We show how the studies of ice cover of continental water bodies can benefit from the synergy of more than 15 years-long simultaneous active (radar altimeter) and passive (radiometer) observations from radar altimetric satellites (TOPEX/Poseidon, Jason-1, ENVISAT and Geosat Follow-On) and how this approach can be complemented by SSM/I passive microwave data to improve spatial resolution. Five largest Eurasian continental water bodies - Caspian and Aral seas, Baikal, Ladoga and Onega lakes are selected as examples. First we provide an overview of ice regime and history of ice studies for these seas and lakes. Then a summary of the existing state of the art of ice discrimination methodology from altimetric observations and SSM/I is given. The drawbacks and benefits of each type of sensor and particularities of radiometric properties for each of the chosen water bodies are discussed. Influence of sensor footprint size, ice roughness and snow cover on satellite measures is also addressed. A step-by-step ice discrimination approach based on a combined use of the data from the four altimetric missions and SSM/I is presented, as well as the results of validation of this approach using *in situ* and independent satellite data in the visible range. The potential for measurement of snow depth from passive microwave observations using both altimeters and SSM/I is addressed and a qualitative comparison of *in situ* snow depth observations and satellite-derived estimates is made.

Keywords

radar altimetry, radiometry, ice and snow cover, Caspian sea, Aral sea, Lake Baikal, Lake Onega, Lake Ladoga

Introduction.

Many boreal continental water bodies have seasonal ice cover. In this work we address ice conditions in five largest Eurasian continental water bodies - Caspian and Aral seas, Baikal, Ladoga and Onega lakes (Figure 1) that every year are covered by ice for several months. Ice cover dramatically affects energy exchange between water and atmosphere, hydrophysical and hydrobiological processes in these seas and lakes. Living conditions of endemic mammals, such as Baikal and Caspian seals, that use ice to pup, nurse, mate and molt [Pastukhov, 1993; Kouraev et al., 2004a, 2007a], strongly depend on ice conditions. Ice dynamics influences transport and navigation, fisheries and other industrial activities, such as Russian and Kazakh oil prospecting rigs operating on the Northern Caspian shelf. Temporal and spatial variability of ice processes in these seas and lakes is influenced by meteorological conditions (mainly by thermal regime), but also by wind and currents, bottom morphology and other factors. Studies and monitoring of ice cover conditions are thus providing valuable information for climate research, maritime safety and sustainable environmental management.

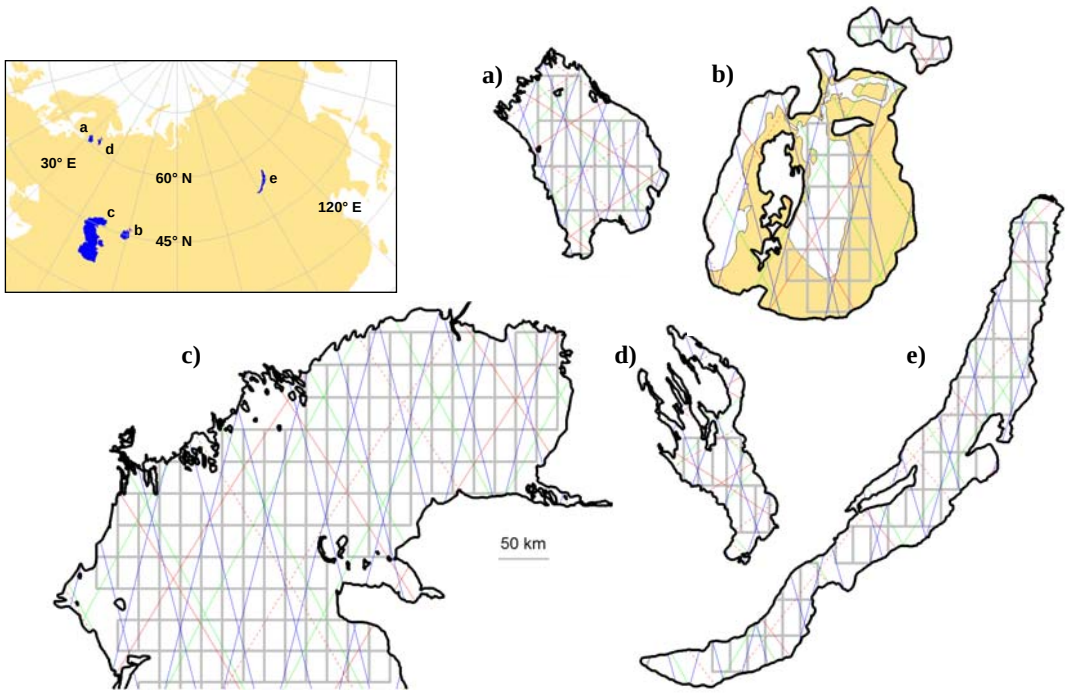

Figure 1. Selected continental water bodies: a) Ladoga lake, b) Aral sea (black line - coastline position in 1992, yellow region - area dried out between 1992 and October 2006), c) Northern Caspian sea, d) Onega lake, e) Baikal lake. Also shown are satellite tracks for radar altimeters (red lines - T/P and Jason-1, dotted red lines - T/P new orbit, blue line - ENVISAT, green line - GFO) and selected SSM/I EASE-Grid pixels (grey rectangles) are also shown. All water bodies are presented in the same scale.

As for many large continental water bodies, for these five natural objects observations of ice regime have started in the end of the 19th - beginning of the 20th century at coastal stations. Later on, mainly between 1940ies and 1970ies, field trips and aerial surveys made it possible to significantly extend the research from point observations to lake- or sea-wide spatial scale. However, the high cost of aerial observation led to significant decrease of number of observations

since the end of 1980ies. The lack of aerial surveys has been complemented by the use of satellite remote sensing data, mostly in the visible range. However, these observations depend on the availability of solar light and are affected by the presence of cloud cover, often present over these water bodies.

Microwave satellite observations represents a step forward, providing reliable, regular and weather-independent data on ice cover. For the last 30 years the scientific community has extensively used passive microwave data from the SMMR (Scanning Multichannel Microwave Radiometer, 1978-1987) and the SSM/I (since 1987) instruments to estimate ice cover extent and type (first-year and multi-year ice) both in the Arctic and in the Antarctic. Passive radiometric data have also been successfully combined with optical and infrared observations from other satellites [Emery et al., 1994]. During the 1984 Marginal Ice Zone Experiment (MIZEX) ice cover has been studied using simultaneous observations from passive (radiometers) and active (SAR) sensors during aircraft flights [Burns et al., 1987; Cavalieri et al., 1990]. First studies of sea ice using simultaneous active and passive observations from the same satellite platform have been made using 14 months of data (1995 to 1997) from OKEAN-01 satellite radiometer RM-08 (36.62 GHz frequency, spatial resolution 15x20 km) and side-looking X-band (3.1 cm) radar RLS-BO (spatial resolution 1.5x2 km data), and an ice concentration algorithm using a linear mixture model has been proposed [Belchansky and Douglas, 2000, 2002].

These combination of passive and active observations have been using sensors with different spatial resolution and different incidence angle. With the launch of series of radar altimeter satellites, scientific community have now continuos and long time series of both active (radar altimeter) and passive (radiometer used to correct altimetric observations) simultaneous observations, from the same platform and with the same incidence angle (nadir-looking).

Although the primary mission of satellite altimetry is the study of water level of the open ocean, this technique have been successfully applied for continental surfaces to monitor water level of inland seas such as Caspian and Aral seas [Cazenave et al., 1999; Aladin et al., 2005, Crétaux et al., 2005], large lakes [Ponchaut and Cazenave, 1998; Mercier et al., 2002, Crétaux and Birkett, 2006], as well as large rivers, wetlands and floodplains [Birkett, 1998; de Oliveira Campos et al., 2001, Maheu et al., 2003]. Satellite altimetry has been applied not only to derive river level, but also to reconstruct river discharge from the Ob' and Amazon rivers [Kouraev et al., 2004c, Zakharova et al., 2006]. Satellite altimetry for sea ice studies started with the Seasat altimeter in 1978, and used the variability of the radar backscatter over the ice [Fetterer et al., 1992]. Recent studies use satellite altimeter measurements to estimate the ice freeboard and assess ice thickness in the Arctic [Laxon et al., 2003].

However, these approaches use data only from the radar altimeter. In this work we show how the studies of ice cover on continental water bodies can benefit from the synergy of more than 15 years-long simultaneous nadir-looking active (radar altimeter) and passive (radiometer)

observations from radar altimetric satellites (TOPEX/Poseidon, Jason-1, ENVISAT and Geosat Follow-On) and how this approach can be complemented by passive microwave data (such as SSM/I) to improve spatial resolution.

In section 1 we provide an overview of ice regime and history of ice studies for the selected two saltwater (Caspian and Aral seas) and three freshwater (Baikal, Ladoga and Onega lakes) water bodies. We summarise the existing state of the art of ice discrimination methodology from altimetric observations (Section 2) and SSM/I (Section 3). We discuss the drawbacks and benefits of each type of sensor and particularities of radiometric properties for each of the chosen water bodies. Influence of sensor footprint size, ice roughness and snow cover on satellite measures is also addressed. We present a step-by-step ice discrimination approach based on a combined use of the data from the four altimetric missions and SSM/I, and the results of validation of ice discrimination methodology using *in situ* and independent satellite data in the visible range. In Section 4 we address the potential for measurement of yet another parameter - snow depth - from passive microwave observations using both altimeters and SSM/I, and present a qualitative comparison of *in situ* snow depth observations and satellite-derived estimates.

1. Ice conditions and studies of ice cover for chosen water bodies.

1.1 Ice cover and ice conditions.

1.1.1. Northern Caspian sea. For the large Caspian Sea, only in its shallow northern part called Northern Caspian sea (depths less than 10 m, average depth 5-7 m) ice is present every year and covers large areas. Large surface (88 500 km^2) and small depth of the Northern Caspian lead to an intensive interaction of ice cover with the sea bottom and rapid changes in sea level during storm surges. The presence of ice affects navigation, fisheries and other industrial activities in the Northern Caspian sea, calling for use of ice-breaker fleet in winter. Of special concern is the impact of sea ice on industrial structures located in the coastal zone and on the shelf, such as Russian and Kazakh oil prospecting rigs.

During moderate winter conditions, ice formation starts in November, and by December ice cover is present on all areas of the Northern Caspian with depths less than 5 m. Further development of ice cover is limited by larger depths and increased water exchange with the warmer Middle Caspian. Strong winds often result in intensive deformation of the ice cover and subsequent cracking, fracturing, rafting, as well as the formation of hummocks and ridges. Some hummocks become anchored on the ground, reaching 2-4 m (in some cases - 6 m and more) height [Terziev et al, 1992]. Snow cover on ice is not deep, in February 1991 maximal observed depth was 12 cm in the Northern part, while in the western it was smaller and in the southern part ice was completely snow-free [Lobov et al., 1993; Tsytsarin et al., 1999]. Ice decay starts in March and by April the last ice resides only over the Ural furrow in the north-eastern part. On average, the duration of the

ice period is 120-140 days in the eastern part of the Northern Caspian and 80-90 days or less in the western part.

1.1.2. Aral Sea. The Aral sea is well known by dramatic changes of sea level during the 20th century [Bortnik and Chistyaeva, 1990]. The Aral sea level was relatively stable until the early 1960s, but since river water consumption for agricultural purposes led to 13 m drop in sea level and 40% decrease in sea surface by 1987. Since 1988 the sea was divided onto two separate basins: the Small Aral in the north and the Great Aral in the south (surface in October 2006 was 3200 km^2 and 12300 km^2, respectively). Since 1992 several attempts to build a dam between the Small and Great Aral have been undertaken with the purpose of filling again the Small Aral [Crétaux et al., 2005]. This has resulted in different variability of sea level in those two basins [Aladin et al., 2005, Crétaux et al., 2005, Kouraev et al., 2008]. The Large Aral itself, due to continuing sea level decrease, presently consists of two distinct basins - deepwater western and shallow eastern one - connected through a narrow (~ 3 km) and shallow (~ 3 m) channel**.** Changes in sea level greatly influence ice conditions through changes in the heat storage amount, water exchange and circulation [Bortnik and Chistyaeva, 1990; Ginzburg et al., 2003, Kouraev et al., 2008].

According to historical observations made up to mid-1980ies (before the sea division), the ice conditions were the most severe in the northern and eastern parts of the sea. The ice formation usually began in the coastal regions in mid- November, in the open sea by the end of December, while in the western coastal zone ice formed only in the beginning of January. Variability of the dates of ice formation onset varied from 1 to 2 months depending on the region. The maximal development of ice cover was in February, when, in severe winters, ice may cover the whole sea surface. Average snow depth on ice was 3-6 cm, maximal depth was observed in January and could reach 10-20 cm [Bortnik and Chistyaeva, 1990]. Snow accumulation is typical for uneven or wet ice surface; when ice surface is dry snow is easily blown away. For example, field observations in February 1986 showed, that most of the Aral sea ice was snow-free, in places when snow was observed its depth was less than 1 cm [Tsyzarin 1987, Bortnik and Chistyaeva, 1990]. In February 1990 snow depth varied from 0.5 to 11 cm [Tsytsarin et al, 1993, 1999].

Ice decay started in the end of February - beginning of March and one month later the sea was ice-free. However, in severe winters ice could reside until the end of April or the beginning of May. The number of days with ice ranged from 120-140 days in the north to 100-110 in the south, while in the western regions it was minimal - 70-80 days.

1.1.3. Lake Baikal. This is the deepest lake in the world, representing one fifth of the world's unfrozen freshwater resources. Bathymetric features separate the lake into three distinct basins: two deep-water Southern and Middle (about 1461 and 1642 m, correspondingly [The INTAS Project 99-1669 Team, 2002]) and relatively shallow (depths up to 904 m) Northern Baikal. Different parts of the lake have specific systems of atmospheric circulation, precipitation and

currents, stressing the need for lake-wide ice monitoring [Semovski and Mogilev, 2003; Kouraev et al., 2008a, b].

Lake Baikal region has strongly continental climate conditions; long and cold winters result in the complete freeze-up of the lake every year for 4-5 months. According to historical data [Verbolov et al., 1965; Atlas of the Lake Baikal, 1993] ice formation starts in late December - early January in the Northern Baikal and in the first half of January in the Southern Baikal. Ice break-up starts in early-May in the Southern part of the lake, and in mid-May in the north.

Following the precipitation pattern, maximum snow depth is observed near the south-western coast in Southern Baikal, where snow depth reaches 40 cm on the coast and 20-30 cm in the coastal zone [Atlas of the Lake Baikal, 1993]. Middle Baikal, where precipitation is low, has the minimal snow depth. In the Northern Baikal, where snow redistribution by wind is less than in Middle or Southern Baikal, the whole region is usually covered by snow, and the maximum values are observed along the eastern coast and in the northernmost part of the lake (up to 80-100 cm [Galaziy, 1987]).

The state of the lake ice cover and snow its overlying determine the formation of different hydrophysical fields and influences spring bloom of diatoms and primary productivity [Granin et al., 1999; Semovski et al., 2000; Mackay et al., 2003, 2005]. Due to the high transparency of the Baikal ice, during late winter and early spring, when the lake is still ice-covered, intense development of phytoplankton, zooplankton and benthos starts under the ice. The ice cover is also important for ice transport, fishing activities and tourism.

1.1.4. Lake Ladoga. This is the largest freshwater lake in Europe with a total area of 17 700 km^2, average depth 47 m and maximal depth 230 m. The lake is ice-covered for more than half of the year (from the beginning of November until the end of May) [Hvorov and Utin, 2002]. The first ice on Ladoga is formed in the shallow south-western Petrokrepost Bay. Then it appears along the southern coast and spreads along the eastern coast north up to Mantsinsari Island. The water along the western coast and the northern deep-water zone are the last to become ice-covered. Water over the deep-water area (depths more than 140 m) of the lake remains ice-free for a long time, and sometimes this area does not become ice-covered at all. In this area an intense hummocking is observed as a result of ice drift and movement of ice fields during freeze-up. Lake Ladoga ice cover is usually covered by snow, snow depth varies from several to 20-25 cm. In spring, wind breaks the floating ice and, depending on the wind direction, the ice drifts onshore where it melts. A small part of ice is driven to Petrokrepost Bay and then enters the Neva River. Ice conditions affect navigation on the lake, especially to the popular touristic destinations - monasteries of Valaam and Konevitz in the northern part of the lake.

1.1.5. Lake Onega is the second largest European freshwater lake (surface 9789 km^2). Northern deepwater part of the lake (maximal depth 119 m) has complicated and contrasted coastline and

bottom topography. Southern part is shallow (depths less than 20 m), coastline is weakly dissected. Average lake depth is 27.3 m. 52 rivers flow to the lake, and only one - Svir' river - flow out from the lake, connecting it to the neighbouring Lake Ladoga. Since 1953 Lake Onega became a reservoir with multi-year flow regulation by Upper-Svir' hydropower station. From December to May the lake is partially or completely ice covered.

Both Ladoga and Onega are dimictic lakes, i.e. they are mixed top to bottom twice per year in autumn and spring. Water cooling starts simultaneously over the whole surface of the lakes. After autumn isothermal conditions, further water cooling down to °C takes a long time. Dates of water temperature transition through 0°C between shallow and deep-water regions differ by 1.5-2 months.

1.2. History of studies of ice conditions

1.2.1. Caspian and Aral seas. Studies of sea ice from the coastal stations have begun in the second part of the 19th century for the Caspian Sea, and in 1941 for the Aral sea. In the second part of the 20th century ice studies became part of the Soviet Union's national hydrometeorological monitoring system and were performed on a regular basis using aerial surveys. However, starting from the late 1970ies, the high cost led to a dramatic decrease of aerial ice cover observations. The lack of information was partially compensated for by the use of satellite imagery, mainly in the visible and infrared range [Krasnozhon and Lyubomirova, 1987; Buharizin et al. 1992]. The majority of satellite-based ice maps were made in the 1980s, using data from low-resolution Soviet weather satellites such as “Meteor”. Due to frequent cloud cover in the winter satellite observations have been used only occasionally. As a result, published continuous time series of various ice cover parameters for the Caspian and Aral seas stopped in 1984-1985.

Recent oil prospecting activities in the Russian and Kazakh sectors of the Northern Caspian have led to increase of funding for ice surveys. Currently, Hydrometeorological Service of the Caspian Fleet uses data from NOAA, Meteor-3M and Radarsat-1 satellites. Every year since 2000, team of researchers from the Arctic and Antarctic Institute (AARI), St. Petersburg perform hummock studies in the Northern Caspian. In February-March they effect daily helicopter flights from Astrakhan' to the oil prospecting zone in the Russian sector. In the Kazakh sector ice surveys are also performed using helicopters and field works. However, results of these observations are not available for wide public.

Daily maps of ice concentration in the Northern Caspian sea using the ASI algorithm [Spreen et al., 2008] from AMSR-E (6.25 km) and from SSM/I (12 km spatial resolution) passive microwave data are provided at the website of the Institute of Environmental Physics (IEP), University of Bremen [online archive accessible through IEP sea ice website, 2008]. These maps are available since 2003, partly since 2002 [G. Heygster, personal communication]. In general, passive microwave data provide reliable estimates when the ice cover is developed, but are prone to errors

during ice formation and melting. While the ASI algorithm and the resulting ice maps have been validated for several regions [Spreen et al. 2005, 2008], for the Caspian sea, due to lack of validation data, these ice maps are not yet fully validated. Together with IEP researchers we plan to perform an intercomparison study of the Northern Caspian ice regime from both methodologies - ASI and the one presented in this paper.

1.2.2. Lake Baikal ice cover and other natural conditions have been studied extensively for more than a century [Verbolov et al., 1965; Atlas of Lake Baikal, 1993, Shimaraev et al., 2002b; Wüest et al., 2005]. The existing data (mostly from the Listvyanka coastal station in the Southern Baikal, that has records going back to 1869) have been used for various climatic studies, relating ice conditions in the southern Baikal with global climatic variability [Livingstone, 1999; Magnuson et al., 2000; Todd and Mackay 2003, Shimaraev et al., 2003]. Lake-wide study of ice cover has been done using aerial surveys and field expeditions. However, as for the Caspian and Aral seas the number of observations has sharply decreased since the mid-1980s. The lack of *in situ* information was compensated later by the use of satellite data, such as AVHRR (Advanced Very High Resolution Radiometer) onboard NOAA (National Oceanic and Atmospheric Administration) polar-orbiting satellites, MODIS (Moderate Resolution Imaging Spectroradiometer) onboard the Terra and Aqua satellites, as well as some limited ERS SAR (Synthetic Aperture Radar) images [Semovski et al., 2000; Semovski and Mogilev, 2003]. Since December 2002, a satellite receiving station in Irkutsk is obtaining optical imagery from the MODIS sensor [Irkutsk RICC website, 2005].

1.2.3. Lake Ladoga and Onega. The spatial distribution of ice over Lake Ladoga has been observed regularly using aircraft surveys by the Hydrometeorological Service from 1943 until 1992 [Medres, 1957; Lebedev & Medres, 1966]. Satellite images in the visible, infrared and microwave channels have been used since 1971 [Chizhov and Borodulin, 1984; Usachev et al., 1985]. Recently, NOAA and MODIS satellite images became the main sources for studying ice cover of the Ladoga lake to complement *in situ* observations. Karetnikov and Naumenko (2008) have recently used aerial and satellite observations for 1943-2006 (with the gaps in the observations between 1992 and 1996), where they analysed about 1000 ice concentration grids and proposed a Relative Ice Cover Index to study ice conditions of the Lake Ladoga. Regular aerial surveys of Lake Onega ice cover started in 1955. Stepanova (1962) using data from 76 aerial surveys done between 1955 and 1961 analysed Lake Onega ice processes and suggested method for their forecast. In the 1990ies aerial surveys of Lake Onega ice stopped and since then satellite remote sensing data have been used.

1.2.4. Studies of ice cover using altimetric and radiometric data

For all the five natural objects the end of regular aerial surveys was critical for continuity and homogeneity of ice surveys and we observe many gaps in the ice conditions characteristics since end of 1980ies - beginning of 1990ies. This lack of information was in some degree compensated by the use of satellite imagery in the visible range. However, this approach is limited due to the

frequent presence of cloud cover and short period of sun light in the winter. Microwave data have significant advantages comparing to data in the visible range and can be successfully used alone or together with visible data.

Here we present ice discrimination approach, based on synergy of active and passive microwave data from satellite radar altimeters (TOPEX/Poseidon, Jason-1, ENVISAT and Geosat Follow-On) complemented by SSM/I passive microwave data. This approach has been initially developed and tested for the Caspian and Aral seas and recently also lake Baikal. In [Kouraev et al., 2003] data from the two T/P tracks over the Caspian and Large Aral sea for 1992-2002 have been used to estimate a) dates of ice formation and break-up, b) ice duration and c) percentage of ice presence in the altimetric data. In [Kouraev et al., 2004a, 2004b] the T/P data have been complemented by the SSM/I observations with a dedicated ice/water discrimination approach. Using the satellite datasets for Caspian and Large Aral, two separate time series of ice formation and break-up and ice duration have been obtained. Ice presence has also been calculated - as percentage of ice presence in the altimetric data (same as in [Kouraev et al., 2004b]) and also as total and maximal numbers of ice pixels for various sub-regions of the Caspian and Large Aral sea.

Later on, this approach has been extended to a) complement the T/P observations by Jason-1, GFO and ENVISAT data, and b) provide better spatial and temporal resolution using an improved ice discrimination approach, that combines all altimetric and SSM/I data. This approach has been implemented for the lake Baikal [Kouraev et al., 2007a] and Large and Small Aral seas [Kouraev et al., 2008]. Using this approach, new improved time series of ice events (ice formation, break-up and duration) for the longest possible period (since 1991/1992) for various regions of Lake Baikal and Aral sea have been obtained. Basing on these time series for lake Baikal and air temperature data, analysis of how ice regime is influenced by air temperature and dynamic (wind field, currents) and other (bathymetry, precipitation, etc.) factors has been done [Kouraev et al., 2007b].

In the next three sections we provide a comprehensive assessment of the ice discrimination methodology from altimetric observations and SSM/I. Using the data for the five selected water bodies we discuss the application of this methodology its particularities related with satellite sensors and specific features of each natural object.

2. Satellite data

Satellite altimetry. Data from four radar altimetry missions have been used (Table 1, Figure 1). The earliest data are available from the TOPEX/Poseidon (T/P) satellite, operating since 1992. Since February 2002 T/P have been followed by Jason-1 (on the same orbit). In August 2002, T/P was manoeuvred onto a new orbit, flying halfway between its previous tracks, and provided data until the end of its mission in October 2005. The T/P and Jason-1 data are complemented by observations from radar altimeters onboard Geosat Follow-On (GFO) (since January 2000) and ENVISAT (since November 2002) satellites.

All four altimeters have two main nadir-looking instruments – a dual-frequency (single-frequency for GFO) radar altimeter operating in Ku (13.6 GHz), C (5 GHz) or S (2 GHz) bands, and a passive microwave radiometer operating at two or three frequencies (see Table 1). The fact that these are simultaneous observations from the same platform significantly enhances the data analysis capability (see section 3.1). The repeat period ranges from 10 days for T/P and Jason-1 to 35 days for ENVISAT. The use of 1Hz data provides an along-track ground resolution of about 6 km.

SSM/I data. The passive microwave SSM/I (Special Sensor Microwave/Imager) on board the DMSP (Defence Meteorological Satellite Program) with incidence angle ranging from 50.2 to 52.8 degrees provide measurements of brightness temperature at different frequencies and at different (vertical or horizontal) polarisation (see Table 1). The National Snow and Ice Data Center (NSIDC) provide the SSMI data mapped onto an Equal-Area Scalable Earth Grid (EASE-Grid) projection with 628 km^2 spatial resolution [Armstrong et al., 2003]. The initial data were averaged to obtain pentad (5-day) mean values to provide continuous spatial coverage. We have used SSM/I data starting from 1992 (the beginning of the T/P mission). Altimetry and radiometry data were obtained from the Centre for Topographic studies of the Oceans and Hydrosphere (CTOH) at the LEGOS laboratory.

Table 1. Main parameters of satellite altimetry and radiometry missions.

Satellite	Radar altimeter, band*	Radiometer frequencies, GHz	Cycles used	Time	Repeat cycle, days
TOPEX/Poseidon (T/P) (T/P new orbit)	C,Ku	18,21,37	1-365 (368-446)	Sep 1992 - Aug 2002 (Sep 2002 - Oct 2004)	10
Jason-1	C, Ku	18,21,37	1-209	Feb 2002 - Sep 2007	10
ENVISAT	Ku and S	18.7, 23.8, 34	9-59	Nov 2002 - Jun 2007	35
Geosat Follow-On (GFO)	Ku	22, 37	37-202	Jan 2000 - Oct 2007	17
SSM/I	no	19.35 (H,V), 22.235, 37.0 (H,V), 85.5 (H,V)		Jan 1992-Dec 2004	5

* *Ku band - 13.6 GHz, C band - 5 GHz, S band - 2 GHz.*

3. Ice discrimination from altimetric data

3.1. Ice discrimination from simultaneous active and passive microwave data.

The main instrument onboard altimetric satellites is the radar altimeter and its primary mission is to measure sea level. However, the combination of simultaneous active (radar altimeter) and passive (radiometer) microwave measurements can be successfully used to study ice cover. The ice discrimination method was initially developed for the T/P data on the example of Caspian and

Aral seas and is described in detail in [Kouraev 2003, 2004a, 2004b]. Later on it was expanded to include three other altimetric missions (Jason-1, ENVISAT and GFO) for the lake Baikal [Kouraev et al., 2007a, 2007b]. Here, by expanding the dataset for two seas and three lakes, we provide a comprehensive assessment of ice discrimination algorithm and its application for the five selected water bodies.

This method is based on the analysis spatio-temporal evolution of observations in the space of two parameters. The first parameter is the backscatter coefficient ($\sigma 0$), which is the ratio between the power reflected from the surface and the incident power emitted by the onboard radar altimeter, expressed in decibels (dB). We use backscatter at the Ku band (13.6 GHz). The second parameter is the average value of the brightness temperature values at two frequencies (18 and 37 GHz for T/P and Jason-1, 18.7 and 34 GHz for ENVISAT and 22 and 37 GHz for GFO) measured in ºK, which we call TB/2 [Ulaby et al., 1986]. Open water has a low backscatter coefficient and low brightness temperature values, while ice cover is characterised by a high backscatter coefficient and elevated brightness temperatures.

Temporal evolution of the altimetric observations in the space of backscatter versus TB/2 is presented on Figure 2. One cluster (observations in the lower left corner) with low backscatter coefficient (about 10 dB) and low brightness temperature (TB/2 between 150-160 °K) is always present and represents open water. In November first appearance of young ice leads to some observations with high (30-40 dB) backscatter but still low TB/2. Further development leads to the formation of a cluster of observations typical for sea ice: high backscatter coefficient (mainly 20-30 dB, sometimes up to 40 dB) and high brightness temperatures (TB/2 about 220-260 °K). Maximal ice development is observed for January, in February-March number of observations for ice cluster decreases and in April the sea becomes ice-free.

As a result, annual observations in the space of backscatter and TB/2 form two well-defined clusters (Figure 3a). It is important to note that the use of only one of these parameters (either backscatter coefficient or TB/2) would leads to ambiguities, for example when backscatter is between 20 and 30 dB or when TB/2 is between 190 and 210 °K. But by using simultaneous observations of the two parameters it is possible to distinguish between open water and ice with a high degree of reliability.

Observations from the three other satellite altimetry missions (Jason-1, ENVISAT and GFO) show similar distribution (Figure 3, b-d for the Northern Caspian; the distribution of data from altimetric satellites is similar for each specific water body), again yielding two distinctive clusters corresponding to open water and ice. However, the quality control routines used by the data processing and distributing agencies filter out some observations. There are no data with backscatter values higher than 33 dB for Jason-1 and higher than 31 dB for GFO. For Jason-1 almost all the data acquired over the ice are not provided in the Geophysical Data Records (GDRs), except some observations with low backscatter and high TB/2 (Figure 3 b). This filtering

reduces the accuracy in estimating the timing of ice formation and break-up. In our studies we use Jason-1 data to reliably detect open water. In the future, access to the unfiltered Jason-1 data could provide information for both ice and open water conditions.

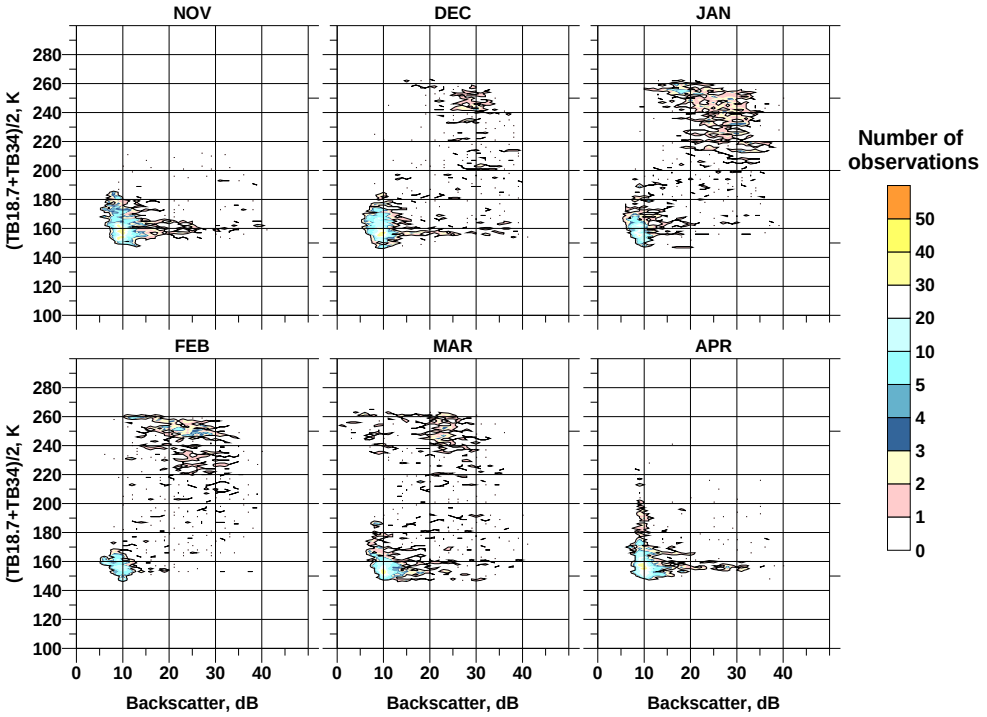

Figure 2. Two-dimensional monthly histograms (number of cases) of ENVISAT observations (cycles 9 to 59) for the Northern Caspian sea in the space of backscatter coefficient (Ku band) versus the TB/2 (average value of brightness temperature at 18.7 and 34 GHz)..

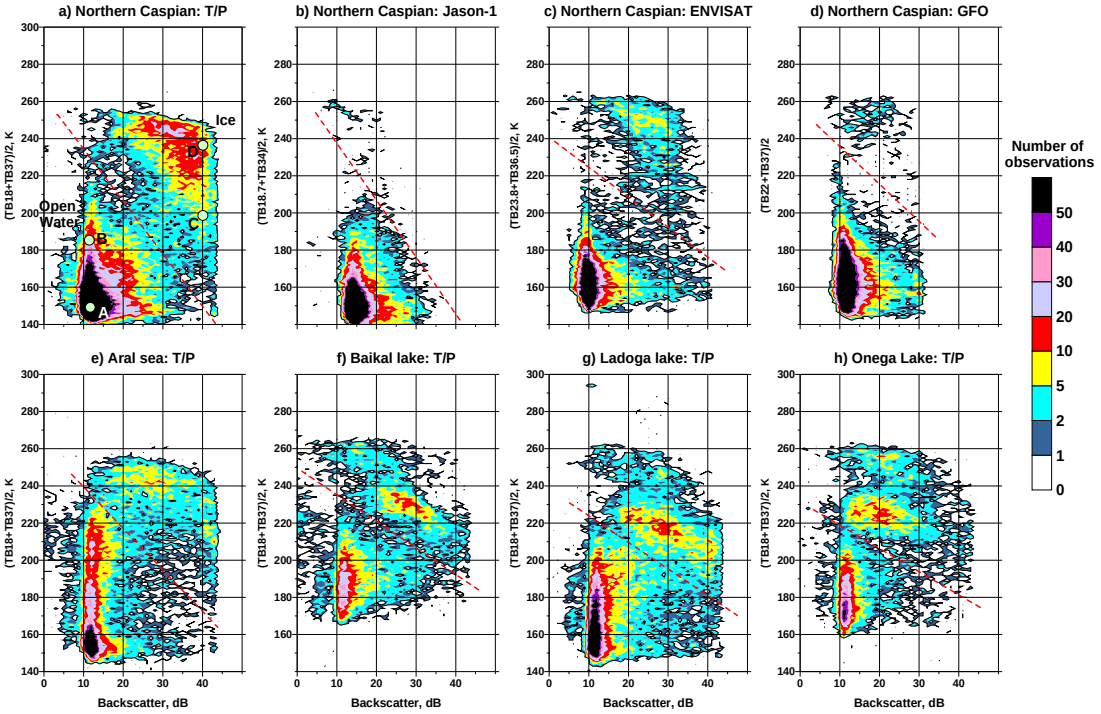

Figure 3. Two-dimensional histograms (number of cases) of observations from T/P (a), Jason-1 (b), ENVISAT (c) and GFO (d) for the Northern Caspian, and observations from T/P for the Aral

sea (e), Baikal (f), Ladoga (g) and Onega (h) lakes. X axis - backscatter coefficient (Ku band), Y-axis - TB/2 (specific for each satellite mission). Red dotted lines illustrate the threshold lines for discrimination between ice and open water. A,B,C and D points on (a) show typical stages of development of radiometric properties (see section 3.2).

Comparison of two-dimensional histograms for the five selected water bodies (Figure 3, a, e-h) shows that the two clusters of open water and ice are always present. The are some similarities and some differences in the absolute values of radiometric properties and in the shape of the two clusters. This behaviour is determined by several factors, such as the footprint size and the temporal variability of the radiometric properties of the ice and snow cover, that are addressed below.

3.2. Influence of footprint size and snow on ice on altimetric observations .

When looking at the distribution of T/P observations in the space of backscatter – TB/2, the influence of the footprint size is important. The average radar altimeter footprint diameter in Ku band is between 10 and 12 km for open ocean (depending on the surface roughness), while the radiometer operating at 18, 23 and 37 GHz has a footprint diameter of 42, 35 and 22 km, respectively. In the case of a heterogeneous surface (mixture of open water and ice) the difference in the spatial coverage will result in different values for the microwave parameters. This issue has been discussed in details in [Kouraev et al., 2004a] where numerical simulation of satellite overfly of various types of surface has been done.

For a situation, when satellite flies from open water (Figure 3a, Point A) toward an ice-covered region (Point D) and crosses the ice edge, its instruments would differently register changes in the backscatter and brightness temperatures. First changes will be observed in the brightness temperature at 18 GHz (largest footprint). This will lead first to slow increase of TB/2 and, with satellite advance, to more rapid one when ice will start influence TB also at 37 GHz. The backscatter values do not change yet and observations are still within the open water cluster (Point B).

When the radar footprint starts to cover the ice edge, both the backscatter and the TB/2 values rise. The measurements rapidly move from open water cluster to ice cluster until the entire radar footprint is over the ice. This corresponds to observations with high backscatter and relatively low TB/2 (some open water is still visible by radiometer) at Point C. As satellite moves further over ice, the backscatter do not change, but TB/2 continues to rise – first rapidly, then (when the entire 37 GHz TB footprint is over the ice) – more slowly, until all footprints see only ice. This corresponds to observations in the upper right corner, with maximal possible values of TB/2 for maximal observed backscatter (Point D).

Once the ice starts growing, it begins to get thicker and more rigid. Wind and currents lead to ice deformation, formation of cracks and ridging, which increases the surface roughness. Snow

accumulates, preferentially near the roughest surfaces.

At the end of the ice season this process is further complicated by melting/refreezing, appearance of pools of water on the ice, and by ice decay. All these processes change the dielectric properties of the ice and thus the microwave signal. In general, ice development, roughening and snow cover decrease the backscatter to 15-20 dB [Ulaby et al., 1986], while TB/2 stays relatively constant or even slightly increase (see fig 3 a, e-h).

Additional information on ice properties, especially when snow cover is present, may be inferred from the differences between passive microwave measurements at different channels. Several snow depth algorithms have been developed for passive microwave data, using a linear relationship between the brightness temperature difference at 19 and 37 GHz to compute snow depth. Marcus and Cavalieri (1998) developed an algorithm that relates snow depth (h_s) over the Antarctic sea ice to brightness temperatures (T_B) at 37 and 19 GHz (vertical polarisation) and ice concentration. For the non-polarised nadir-looking radiometer data from altimetric satellite this relation in the simplified form [Kouraev et al., 2004a] is

$$h_s = -2.34 - 771\frac{T_B(37) - T_B(18)}{T_B(37) + T_B(18)} \quad \text{or} \quad h_s = -2.34 - 771 * GR$$

where GR is the gradient ratio. Since this algorithm was developed for SSM/I that has an incidence angle of 53°, a correction should be taken when using data from the T/P nadir-looking radiometer [Papa et al., 2002].

Absolute values of coefficients are developed for Antarctic and thus not directly transposable for the five selected continental water bodies, but it is important that decrease of GR values is linearly related with the increase of snow depth. Snow cover significantly decreases the backscatter values but it rarely changes the TB/2 values. Thus the lowest GR values correspond to observations located in the far left and lower part of the ice cover cluster for the Northern Caspian (Fig. 4a) and in the far left and upper part of the ice cluster for Ladoga lake (Fig. 4b). Observations in these parts are usually obtained in mid-winter, what corresponds to the maximal snow development over the ice. Moreover, for all freshwater lakes the ice cluster actually separates onto two sub-clusters, separated by TB/2 of 240-245 °K for T/P (Figure 3 f-h), suggesting more developed snow cover than for Northern Caspian and Aral seas.

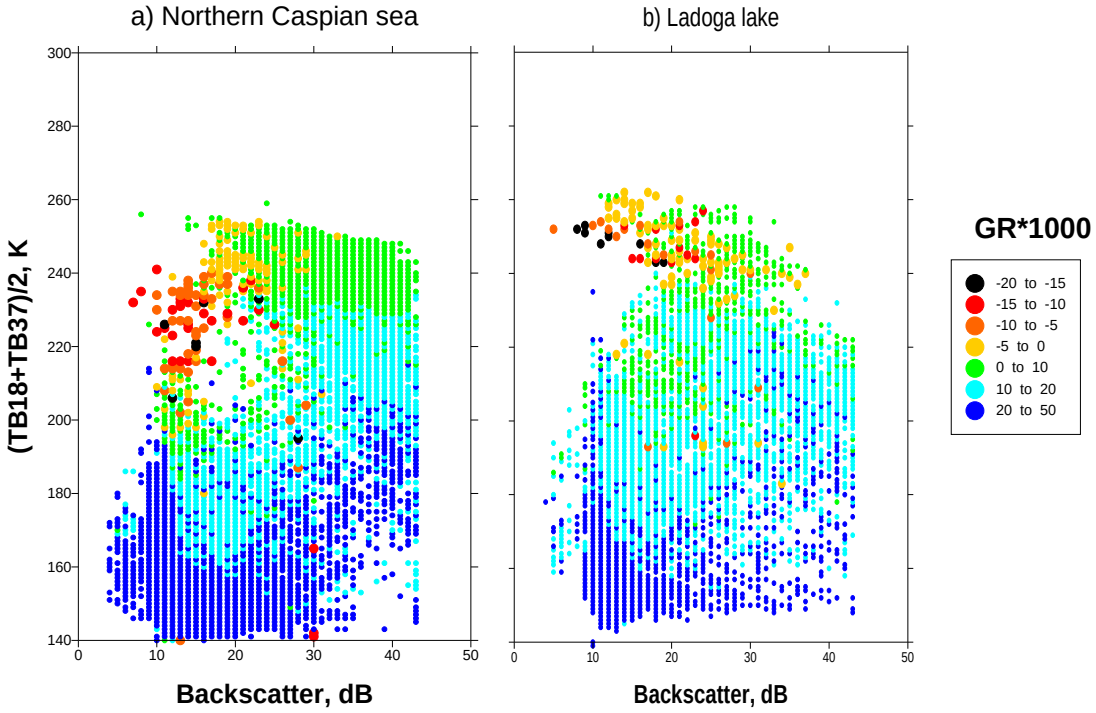

*Figure 4. Mean values of GR*1000 in the space of backscatter vs. TB/2 for the Northern Caspian sea (a) and Ladoga Lake (b)*

3.3. Resulting temporal evolution of altimetric observations.

The specificity of altimetric microwave instruments, footprint geometry, shape and size of the water body, as well as various stages of ice cover development define typical evolution of observations in the space of backscatter vs. TB/2. This development is schematically presented in Fig. 5 for the ensemble of seas and lakes studied. The core of open water cluster is well defined for seas (Point A), though for lakes it is more spread out, probably due to land influence on TB measures (more on this in section 4). Ice formation results first in an increase of TB/2 values (Point B) and then in backscatter values (Point C). If ice cover is visible both in radar and radiometer footprint, both backscatter and TB/2 have high values (Point D). This is the case for seas, but not for the lakes, where observations at point D are rare. As the ice develops and roughens, backscatter decrease and TB/2 increase lead to Point E, where the maximum number of ice cover observations occur. The lower (comparing to seas) TB/2 values at point E could be attributed to land influence on radiometer measurements, while slightly lower backscatter values could be related with ice roughness properties, specific to the three lakes. Snow accumulation, ice ageing and decay induce a further decrease in the backscatter values and changes in brightness temperature leading to point F - maximal snow development. Comparing typical TB/2 values of F and E we see that for seas snow-covered areas have lower TB/2 values, but for lakes this is the opposite. Ice break-up and melting result in a rapid return to points E and then to A (open water).

These features make it possible to use simultaneous active and passive microwave observations

from satellite radar altimeters for discrimination of ice and open water (Section 5) and estimation of snow depth (Section 6).

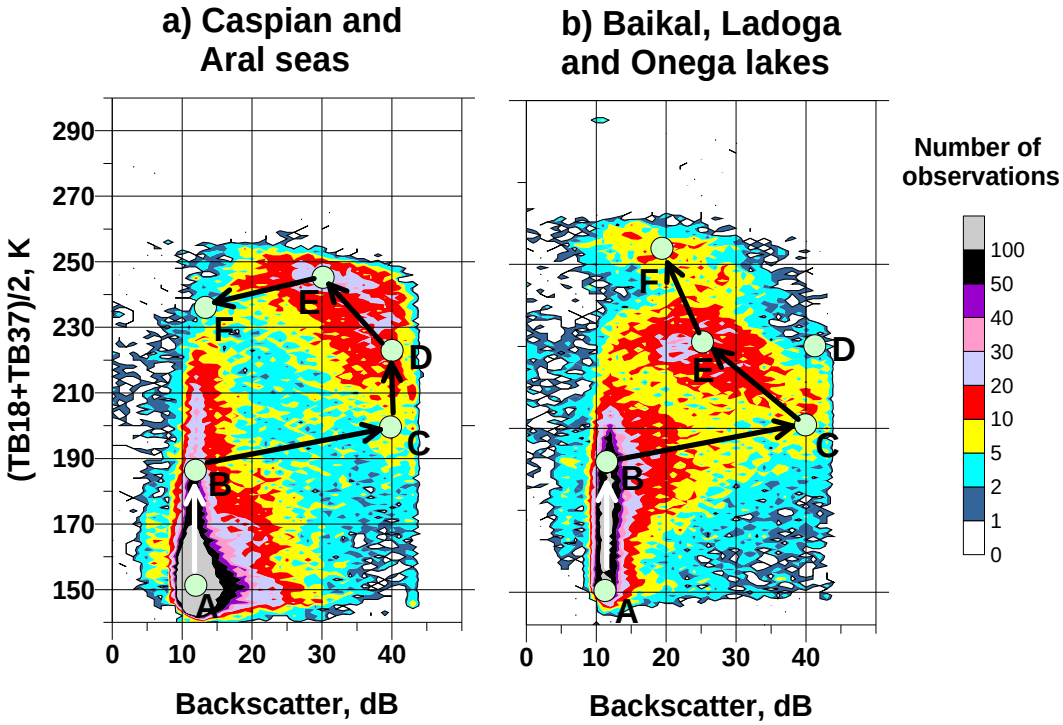

Figure 5. Schematic representation of the temporal evolution of T/P observations in the space of backscatter vs. TB/2. Schema is overlaid on two-dimensional histograms (total summed values) for Caspian and Aral seas (a) and Baikal, Ladoga and Onega lakes (b)

.

4. Ice detection from SSM/I passive microwave data

Among the most commonly used algorithms for estimation of ice concentration from passive microwave data (such as SMMR and SSM/I) are the NASA Team and Bootstrap algorithms [Swift and Cavalieri, 1985; Comiso, 1986; Steffen et al., 1992]. These algorithms use various combinations of brightness temperature (TB) data from the 19.35 (18.0 for SMMR) and 37.0 GHz horizontally (H) and vertically (V) polarised channels. The NASA Team algorithm uses the polarisation (PR) and spectral (GR) gradient ratios, defined as PR=(TB19V-TB19H)/(TB19V+TB19H) and GR=(TB37V-TB19H)/(TB37V+TB19H). Further development of application of passive microwave data from SMMR and SSM/I has resulted in the improvement of the existing algorithms by adding other frequencies (such as 85 GHz) and by development of new algorithms [Svendsen et al., 1987; Marcus and Cavalieri, 2000; Kaleschke et al., 2001].

The use of PR and GR ratios implies a good knowledge of the radiometric properties of various types of surface for each natural object. For Arctic and Antarctic tie points for open water, first-year and multi-year ice has been identified and basing on them estimation of both ice concentration and type are possible [Ulaby et al., 1986; Steffen et al., 1992]. Figure 6 shows the two-dimensional histograms of observations frequency in the PR-GR space for the five selected water bodies, with the tie points for the Arctic ice [Cavalieri, 2008] plotted for comparison (Figure

6 a, c). Though we do not observe multi-year ice in the selected water bodies, the general temporal evolution from open water to smooth ice (first-year ice tie point) to rough ice with snow (multi-year ice tie point) is similar for the Caspian and Aral seas.

However, when using PR and GR parameters for selected continental water bodies we encounter several difficulties. The first one is the absence of *in situ* measurements of radiometric properties of open water and ice parameters for the selection of tie-points. The second - and more important difficulty - is that we seldom observe open water cluster. Only for Northern Caspian (Fig. 6a) we have sufficient number of open water observations, while for other four water bodies open water values have much lower PR ratio and are much closer to the ice cluster. This could be attributed to land-to-water spillover effect (land contamination) related to size and morphology of the selected water bodies. The brightness temperatures come from larger areas than the EASE-grid pixel (628.4 km^2, its height and width varies depending on latitude from about 13.6 x 45.9 km for Onega and Ladoga lakes to 20.4 x 30.7 km for the Northern Caspian), since the original spatial resolution is coarser (69 x 43 km for 19 GHz and 37 x 29 km at 37 GHz). This effect has been analysed in detail by Cavalieri et al (1999) who implemented a land spillover correction algorithm, where a reduction coefficient for sea ice concentration (defined as a function of the closeness of the pixel to the shore) is introduced for the coastal areas. For our five selected water bodies due to the size of the objects almost all SSM/I observations are in some degree affected by land influence, except for the central southern pixels selected for Northern Caspian (Figure 1). The third difficulty is that for freshwater ice (Baikal, Ladoga and Onega lakes, Figure 6 c-e) the angle of evolution between ice and rough ice/snow is different (see red arrows in Fig 6b and d), suggesting different radiometric signatures of ice ageing and development between sea ice and freshwater ice.

We have seen that the combination of simultaneous active and passive data from altimetry missions presents the observations as two distinctive clusters (Fig. 3) and gives the possibility to unambiguously discriminate between ice and open water, observations from SSM/I for the selected water bodies form two mixed clusters and it is sometimes difficult even to distinguish with high degree of confidence between ice and water. As a result, we apply threshold values of PR*100 (9 for Ladoga, 7 for Onega and Baikal lakes, 12 for Northern Caspian and Aral seas) to distinguish between ice and open water (Figure 6, red dotted lines). In general, we consider that altimetry-derived ice cover parameters are of better quality, and SMM/I observations are used to spatially complement the altimeter database.

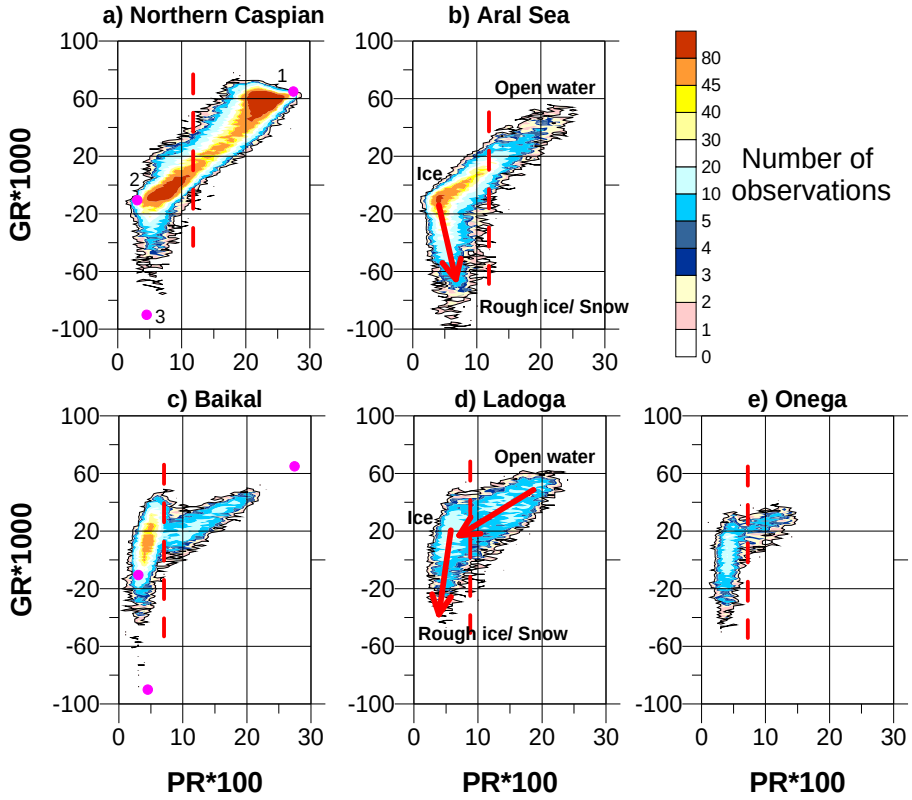

*Figure 6. Two-dimensional histograms (number of cases) of SSM/I winter observations in the space of PR*100 versus GR*1000 for 1992-2007 for a) Northern Caspian and b) Aral seas, c) Baikal, d) Ladoga and e) Onega lakes. NASA Team Arctic tie points for open water (1), first-year ice (2) and multi-year ice (3) are marked on a) and c) as violet circles. Red arrows show the typical temporal evolution of observations for seas (b) and lakes (d) from open water to ice and then to rough ice/ snow. Dotted red line show the selected boundary between open water and ice.*

5 Defining timing of ice events from combination of altimetric and SSM/I data

5.1. Methodology

Basing on the combination of ice discrimination approaches for altimetric (Section 3) and SSM/I data (Section 4) we present here a methodology to define timing of specific ice events over the selected lakes and seas. The whole satellite dataset has been processed in three main steps.

The first step consists in geographical selection of the data. To minimise the potential contamination of the altimetric and SSM/I signal by land reflections, but at the same time to retain a sufficiently large number of altimeter and radiometer measurements over water, a geographical selection of the data needs to be done. For the altimetry data we have excluded data closer than 1 km from the coast, and for the SSM/I data we have excluded EASE-grid pixels when more than 30% of the pixel covers coastal regions or islands. Selected tracks and SSM/I pixels are shown on Figure 1. Compared to SSM/I, the altimetric data are able to enhance the information content due to their high spatial resolution along the track. While the theoretical footprint of the altimeter data is about 12 km (see section 1.1), the main part of the backscatter signal comes from a small area

with a diameter of 1-2 km, which occurs in the case of the quasi-specular signal over ice [Legrésy and Rémy, 1997]. Using MODIS imagery as a reference, high precision of ice edge detection using satellite altimeters has been reported for the Caspian Sea [Kouraev et al., 2003] and for Lake Baikal [Kouraev et al., 2007a].

During the second step we use the two-dimensional histograms for the whole dataset and for each satellite, to graphically define a set of thresholds values (shown as dashed lines on figures 3 and 6) that separate open water from ice. These values are specific for each satellite and for each natural object and do not change with time. Then the threshold values are applied to the satellite data for each pentad to classify all processed altimetric and SSM/I data as either ice or open water.

As the third step, obtained classification is graphically presented as maps for each pentad. Examples of maps and detailed description of their analysis is given in [Kouraev et al., 2007a] on the example of Lake Baikal. By analysing these classification maps for each pentad it is possible to define specific dates of ice events (the first appearance of ice, the formation of stable ice cover, the first appearance of open water and the complete disappearance of ice) for each water body or its sub-region. In some cases the definition of ice event dates could be uncertain due to: a) data gaps for SSM/I or altimetric observations, b) ambiguous ice detection related to land contamination of the microwave signal, and c) consecutive freezing and melting events. In order to account for this uncertainty, for each event it is possible to provide a time span of earliest and latest possible dates, as it has been done for Lake Baikal and Aral sea [Kouraev et al., 2007a, 2008]. Concerning the spatial and temporal resolution of altimetric satellites, the combination of two or more satellites significantly increases the spatial coverage for a given pentad [Kouraev et al., 2007a]. Nevertheless, even one altimetric satellite in combination with SSM/I provides an important contribution to lake ice monitoring. As a result, the pentad-based classification maps always contain SSM/I data and a varying, but significant number of altimetric observations. In most cases it is possible to define ice event dates using these maps with a five-day temporal resolution and an uncertainty of ±2.5 days.

By combining the two types of observations we use their specific advantages – wide spatial coverage and good temporal resolution for SSM/I and high radiometric sensitivity and along-track spatial resolution for altimetry. The combined altimetric-SSM/I observations significantly enhance the capabilities of microwave measurement for ice studies. During the analysis it is good to ensure that both types of data agree with each other; in case of doubt, we suggest to give priority to the altimetric data. Analysis of several consecutive maps usually significantly improves the reliability of the estimates. In some cases the SSM/I pixels near the coast could be subject to potential land contamination such as when ice was observed for one pentad but not observed for the previous or later pentad. If there are no altimetric data to confirm this, we suggest to discard these observations as unreliable.

5.2. Validation of results.

First validation of surface type classification from T/P altimetric observations has been done for the Caspian sea [Kouraev et al., 2003] for the period of ice formation during the winter 2001/2002. Using independent *in situ* ship observations and MODIS satellite image it has been shown that ice formation and movement, as well as ice edge position are very well detected from T/P data. Further validation has been illustrated for Baikal using MODIS imagery for several consecutive dates [Kouraev et al., 2007a]. When the ice cover is well developed both SSM/I and altimetric approaches provide a robust discrimination between water and ice. However, for detecting young and rotten/broken ice, altimetric simultaneous active/passive data are more sensitive than the SSM/I passive data.

This issue has been further analysed in [Kouraev et al., 2007a], where in order to assess the impact of altimetric data in improving ice/open water detection, we have compared ice event dates for Lake Baikal obtained using two datasets: a) SSM/I and altimetric data and b) SSM/I alone. In many cases we did not find any difference. For example, altimetry brings no additional information when the whole lake is ice-covered, or in periods of rapid freezing or melting, when large lake areas undergo simultaneous changes. However, due to signal contamination from land, SSM/I sometimes provides first ice estimates that are too early (up to 25-30 days, 3 cases). or too late (5 to 15 days, 11 cases in total). The dates for 100% ice cover have been similar using both datasets. Observation of the first water is in most cases also unambiguous, but for 100% open water SSM/I alone sometimes give dates that are either too early (5 days, 3 cases) or too late (3 cases, from +10 to +40 days). Once again, this is apparently related to land contamination. This inter-comparison shows that combination of altimetric observations and SSM/I assures high reliability of estimates of ice events dates.

Direct comparison of the ice event dates from satellites and from coastal station observations was possible for Listvyanka station in Southern Baikal [Kouraev et al., 2007a,b]. When comparing satellite estimates and observation at coastal stations it is necessary to bear in mind a) the difference in the methodology of definition of specific ice dates at the coastal stations, and b) the difference between the size of the region observed from the coast and the much larger lake area observed by satellites. However, in spite of these difficulties, for the freeze-up dates the satellite estimates show remarkably good agreement with the *in situ* data. In general satellites define ice formation slightly earlier due to the differences in the observation area. The differences are in the range of 2-6 days except for winter 2002/03 when the difference is 17 days, due to specific ice formation and development character in December 2002 - January 2003 [Kouraev et al., 2007a]. Concerning the ice break-up dates, the *in situ* Listvyanka data estimates of ice break-up are also in very good agreement with the 100% open water dates defined from satellite data (difference of 1-2 days, rarely 7-8 days). Fast ice duration also shows very good agreement between the historical data and satellite-derived estimates, with differences less than five days, except for 1994-1995 and 2002-2004. These results for the Lake Baikal show that ice phenology derived from a combination of active and passive microwave observations from radar altimetric missions and SSM/I can be reliably used to extend the existing time series available for coastal stations, and also to create new

time series for regions which were not previously covered by continuous *in situ* observations.

6 Snow cover from *in situ* data and satellite estimates.

Another promising application of satellite altimetry and radiometry for continental water bodies are studies of time and space variability of snow cover on ice. Snow cover, together with the timing of ice formation and break up are affecting substantially the functioning of the ecosystems in lakes and seas. For example, for lake Baikal the interannual variability of the spring bloom intensity of diatoms is also associated with the character of the snow and ice cover during the wintertime [Kozhova and Izmest'eva, 1998, Granin et al., 1999, Mackay et al., 2003, 2005]. Transmission of incident solar radiation through different types of ice and snow cover can differ by almost an order of magnitude. A dry, cold layer of snow more than 10 cm in thickness reflects as much as 95% of total radiation [Sherstyankin 1975]; therefore, the intensity of radiation that penetrates through the ice is below 10-12 W/m^2, which for some phytoplankton species can be a limiting factor for vital functions [Semovski and Mogilev, 2003].

As it has been discussed in section 3.2, by establishing the relation between GR values from satellite altimeters and radiometers and *in situ* snow depth data one could estimate snow depth over continental water bodies. Unfortunately, snow depth observations over the selected seas and lakes are heterogeneous and for the most part unpublished. Coincident *in situ* snow depth data and satellite observations are very rare and not available to us.

However, at the qualitative level, it is possible to estimate the accuracy of satellite measures for the Lake Baikal. For this lake, one of the few available data on the spatial distribution of snow in the first decade (10-days) of March (figure 7) was acquired during the 1972/73 and 1972/74 winters ["Atlas of the Lake Baikal..", 1993]. The snow depth distribution (see also section 2.1) reflects the general and local features of the atmospheric circulation, as well as the orographic features of the Baikal coast, which is surrounded by mountain ridges. Dominant north-western pattern of precipitation results in maximum snow depth along the ridges of the eastern and south-eastern coasts of lake Baikal. Snow transport across the lake by strong north-western winds lead to increase of snow depth from the western to the eastern coast. As a result, snow depth along the western coasts is low, especially in the Middle Baikal, where winds are the strongest comparing to Southern or Northern Baikal. These measurements reflect the general patterns of snow distribution and they may serve as estimates for typical snow distribution over the lake Baikal in the beginning of March.

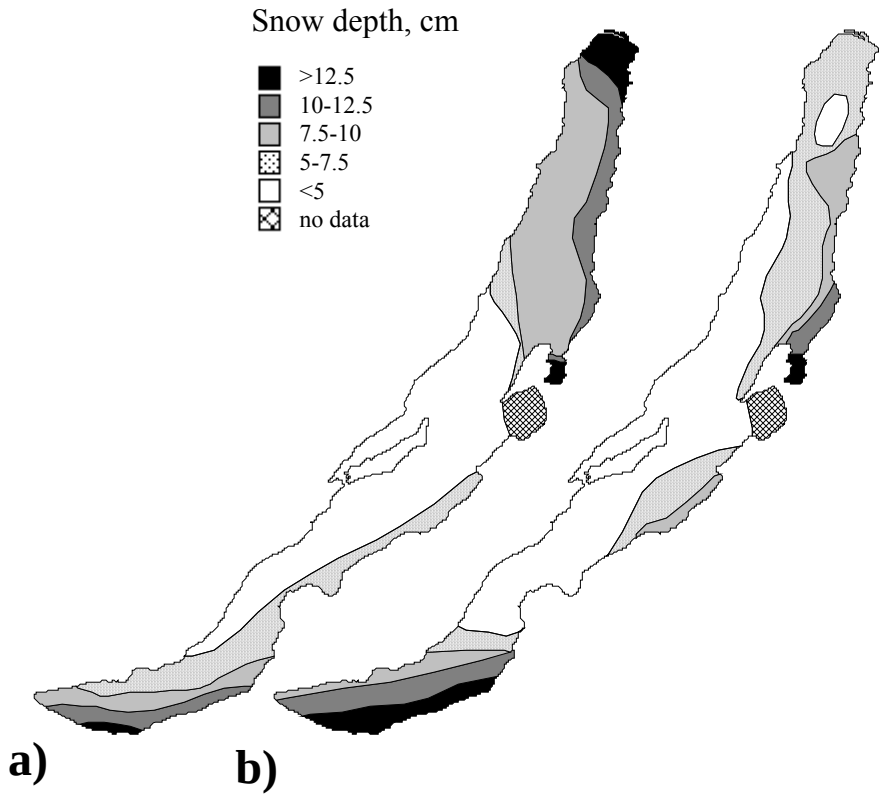

Figure 7. Snow depth (cm) in the first decade (10-day period) of March in 1973 (a) and 1974 (b), after ["Atlas of the Lake Baikal..", 1993].

We have used the SSM/I and T/P brightness temperatures datasets to estimate the spatial GR (from 37 and 19 GHz at vertical polarisation for SSM/I and 18 and 37 GHz for T/P) data variability over the lake Baikal. SSM/I data (figure 8a) indicate very low (less than 5) values of GR*1000 (thus high snow depth) in the northern part of Northern Baikal, as well as low (between 5 and -5) GR*1000 values in the southern Baikal and along the eastern coast of Northern Baikal. Relatively low values are observed for two pixels (third line from bottom) in the region of Selenga delta, probably reflecting land contamination of signal. Highest GR*1000 ratio (from 5 to 20) are observed in the Middle Baikal, where the snow depth is minimal. Compared to SSM/I, T/P data have coarser spatial coverage, but an increased along-track spatial resolution, and they show similar distribution pattern of GR ratio (figure 8b). The lowest values of GR*1000 (not corrected for viewing angle) are observed in the Northern Baikal - from -20 to 0 in the northern tip and on the eastern coast; in the Southern Baikal lower GR*1000 values are observed on the eastern coast; highest values are typical for the Middle Baikal. As a result, typical spatial snow depth distribution in March is well represented by both SSM/I and T/P observations in the passive microwave range.

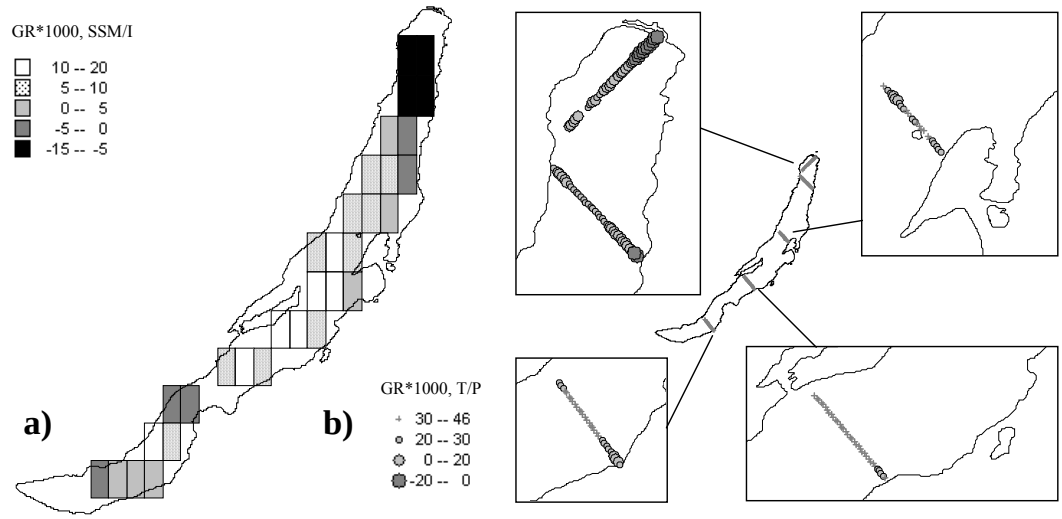

*Figure 8. Spatial distribution of GR*1000 ratio from SSM/I and T/P data. a) average for 1992-2002 values of GR*1000 ratio from SSM/I data for the first decade of March; b) same as in a), but from T/P data. T/P GR values on this figure are not corrected for the difference of viewing angles between SSM/I and T/P..*

We should also bear in mind that passive microwave observations are prone to errors related with the temporal evolution of snowpack during the winter. Variability of snow crystal size affects the GR ratio, and successive snow melt and re-freezing events change the signal, leading to a possible overestimation of the snow depth [Mognard and Josberger, 2002]. In order to reduce snow depth overestimation it is necessary to use more advanced approaches, such as the dynamic snow depth algorithm [Mognard and Josberger, 2002; Josberger and Mognard, 2002], that takes into account temporal evolution of crystal size to correct these estimates.

Conclusions

For all of the five natural objects the end of regular aerial surveys was critical for continuity and homogeneity of ice observations. This lack of information on ice conditions since end of 1980ies - beginning of 1990ies. was in some degree compensated by the use of satellite imagery in the visible range, but this approach has its limitations. Microwave satellite observations in the active and passive range provide reliable, regular and weather-independent data on ice and can be successfully used alone or together with visible data.

The proposed methodology for ice discrimination using simultaneous active and passive data from the four altimetric missions and passive data from SSM/I is very promising. The two types of observations have specific advantages – wide spatial coverage and good temporal resolution for SSM/I and high radiometric sensitivity and along-track spatial resolution for altimetry. The combined altimetric-SSM/I observations significantly enhance the capabilities of microwave measurement for ice studies. The validation of the approach using *in situ* and independent satellite data in the visible range shows very good results.

The proposed methodology can be reliably used to extend the existing time series available for coastal stations, and also to create new time series for different parts of water bodies, which were not previously covered by continuous *in situ* observations. Comparing to ice observations from the coastal stations, satellite data provide observations of the interannual dynamics of ice formation and break-up at the scale of the sub-basin, and in this respect are more representative for ice conditions for large regions of the sea or lake

Data from altimetric satellites and SSM/I has also potential for measurement of yet another parameter - snow depth. In the absence of *in situ* data snow depth data for the period of satellite observations it is not possible actually to establish a statistically sound quantitative relation. But a first qualitative comparison of *in situ* snow depth observations and satellite-derived estimates for Lake Baikal shows promising results.

Acknowledgements

We are grateful for the Center for Topographic studies of the Oceans and Hydrosphere (CTOH) at LEGOS, Toulouse, France for provision of the altimetric and radiometric data. The research has been partly supported by the AICSEX (Arctic Ice Cover Simulation Experiment) Project of the 5th framework program of the European Commission and RFBR (Russian Foundation for Basic Research) Grants No. 04-05-64839 and 03-05-64226. **Any other projects?**

References.

Aladin N, J-F Crétaux, I. S. Plotnikov, Kouraev A. V., A. O. Smurov, A. Cazenave, A. N. Egorov, F. Papa. "Modern hydro-biological state of the Small Aral Sea". Environmetrics, 2005, 16(4), pp 375-392

Armstrong, R.L., Knowles, K.W. , Brodzik, M.J. & Hardman, M.A. (1994, updated 2003). DMSP SSM/I Pathfinder daily EASE-Grid brightness temperatures". National Snow and Ice Data Center. Digital media and CD-ROM. Boulder, CO.

Atlas of the Lake Baikal. (1993). Russian Academy of Sciences, Siberian branch. Moscow: Federal Service of geodesy and cartography 160 pp. (In Russian).

Belchansky, G.I., & Douglas, D.C. (2000). Classification methods for monitoring Arctic sea ice using Okean passive/active two-channel microwave data. J. Remote Sens. Environ. 73, 307-322.

Belchansky, G.I., & Douglas, D.C. (2002). Seasonal comparisons of sea ice concentration estimates derived from SSM/I, OKEAN, and RADARSAT data. J. Remote Sens. Environ. 81, 67-81.

Birkett C. Contribution of the Topex NASA radar altimeter to the global monitoring of large rivers and wetlands. Water Resources Res. 34, 1223-1239, 1998

Bortnik V. N. and S. P. Chistyayeva, Eds., Gidrometeorologiya i Gidrohimiya Morey (Hydrometeorology and Hydrochemistry of Seas). Leningrad, Russia: Gidrometeoizdat, 1990, vol. VII, Aral Sea.

Buharizin, P. I., Vasyanin, M. F. & Kalinichenko, L. A. 1992: Metod kratkosrochnogo prognoza polozheniya kromki splochen nyh ldov na Severnom Kaspii. (A method for short-term forecasting of the pack ice boundary in the northern Caspian.) Meteorologiya i gidrologiya (Meteor-ology and Hydrology) 4, 74–81. Moscow.

Burns, B.A., Cavalieri, D.J., Keller, M.R., Campbell, W.J., Grenfell, T.C., Maykut, G.A., Gloersen, P. (1987). Multisensor comparison of ice concentration estimates in the marginal ice zone. Journal of geophysical research, Vol. 92, No. C7, 6843- 6856

Cavalieri D.J. accessed 2008. NASA Team Sea Ice Algorithm. http://nsidc.org/data/docs/daac/nasateam/index.html

Cavalieri, D.J., Burns, B.A., & Onstott, R.G. (1990). Investigation of the effects of summer melt on the calculation of sea ice concentration using active and passive microwave data. J.

Geophys. Res., Vol 95, No C4, 5359–5369.
Cavalieri, D.J., Parkinson C.L., Gloersen P., Comiso J.C., and Zwally H.J. (1999), Deriving long-term time series of sea ice cover from satellite passive-microwave multisensor data sets. J. Geophys. Res., Vol. 104, No. C7, 15803-15814
Cazenave A., Bonnefond P., Dominh K., Shaeffer P. Caspian sea level from Topex-Poseidon altimetry: level now falling. Geophys. Res. Lett. 24, 881-884.
Chizhov A.N., Borodulin V.V. Kharakteristika prostranstvennogo raspredeleniya tolshiny l'da na Ladozhskom ozere po materialam radiolokazionnoy syemki. (Spatial distribution of ice thickness on Lake Ladoga using radar surveys). Trudy GGI - Proceedings of the State Hydrological Institute, issue 299, Leningrad, 1984. pp. 36-47.
Comiso, J.C. (1986). Characteristics of Arctic winter sea ice from satellite multispectral microwave observations. J. Geophys. Res., vol. 91, 975-994.
Crétaux J. F. and Birkett S., Surface waters from space: lakes. Geosciences Comptes Rendus, Académie des sciences, Thematic issue 'Observing the Earth from space', 2006, 1098-1112.
Crétaux, J-F, A.V. Kouraev, F. Papa, M.Bergé-Nguyen, A. Cazenave, N. Aladin, I.S. Plotnikov. "Water balance of the Big Aral Sea from satellite remote sensing and in situ observations". Journal of Great Lakes Research, 2005, 31(4), p. 520-534.
de Oliveira Campos, Ilce et al. Temporal variations of river basin water from TOPEX/Poseidon satellite altimetry. Application to the Amazon basin. Comptes Rendus de l'Academie des Sciences, Serie II, Sciences de la Terre et des planetes, 333, 1-11, 2001
Emery, W. J., Fowler, C., & Maslanik, J. (1994). Arctic sea ice concentra-tions from special sensor microwave imager and advanced very high resolution radiometer satellite data. Journal of Geophysical Research, 99, 18329-18342.
Fetterer F. M., M. R. Drinkwater, K. C. Jezek, S. W. C. Laxon, R. G. Onstott, and L. M. H. Ulander, "Sea ice altimetry," in Microwave Remote Sensing of Sea Ice, Geophysical Monograph, F. D. Carsey, Ed. Washington, DC: AGU, 1992, vol. 68.
Galaziy, G. I. (1987). Baikal in questions and answers.Irkutsk: Eastern-Siberian publishing (In Russian). (3), 1387-1398.
Ginzburg, A.I., Kostianoy, A.G., Sheremet, N.A., 2003. Thermal regime of the Aral Sea in the modern period (1982-2000) as revealed by satellite data. J. Marine Systems. V.43, 19-30.
Granin, N.G., Jewson, D.H., Grachev, M.A., Levin, L.A., Zhdanov, A.A., Averin, Gnatovsky, R.Yu., Gorbunova, L.A., Tcekhanovsky, V.V., Doroshenko, L.M., Minko, N.P. (1999). Turbulent mixing in the water layer just below the ice and its role in development of diatomic algae in Lake Baikal. Doklady Akademii Nauk, 366, 835-839.
Hvorov, G. V. & G. N. Utin (eds), 2002. Atlas of Lake Ladoga. Limnology Institute of the Russian Academy of Science, Saint-Petersburg (in Russian).
IEP website: Institute of Environmental Physics, University of Bremen, http://www.iup.uni-bremen.de/seaice/amsr/, accessed February 2008.
Irkutsk RICC website, http://geol.irk.ru/bricc.htm.
Josberger, E.G. and N.M., Mognard, A passive microwave snow depth algorithm with a proxy for snow metamorphism, in Hydrol. Process., 16, 8, 1557-1568, 2002.
Kaleschke L., Lupkes, C., Vihma, T., Haarpaintner, J., Bochert, A., Hartmann, J., & Heygster, G. (2001). SSM/I Sea Ice Remote Sensing for Mesoscale Ocean-Atmosphere Interaction Analysis. Canadian Journal of Remote Sensing, Vol. 27, No. 5, 526-537.
Karetnikov S.G., Naumenko M.A. Recent trends in Lake Ladoga ice cover. 2008. Hydrobiologia, in press.
Kouraev A.V., A.G. Kostianoy, S.A. Lebedev. Aral Sea ice cover and sea level from satellite altimetry and radiometry (1992-2006). Journal of Marine Systems, 2008, submitted.
Kouraev A.V., Kostianoy A.G., Lebedev S.A. "Recent changes of sea level and ice cover in the Aral Sea derived from satellite data (1992-2006)". Journal of Marine Systems, 2008, submitted
Kouraev A.V., Papa F., Buharizin P.I, Cazenave A, Crétaux J-F, Dozortseva J, and Remy F., "Ice cover variability in the Caspian and Aral seas from active and passive satellite microwave data". Polar Research, Vol. 22, No 1, 2003, p. 43-50.
Kouraev A.V., Papa F., Mognard N.M., Buharizin P.I, Cazenave A, Crétaux J-F, Dozortseva J, and Remy F. Synergy of active and passive satellite microwave data for the study of first-year sea ice in the Caspian and Aral seas. IEEE Transactions on Geoscience and Remote Sensing (TGARS), vol. 42, No 10, October 2004a, pp. 2170-2176
Kouraev A.V., Papa F., Mognard N.M., Buharizin P.I, Cazenave A, Crétaux J-F, Dozortseva J,

and Remy F. "Sea ice cover in the Caspian and Aral seas from historical and satellite data". Journal of Marine Systems, 47, 2004b, pp. 89-100

Kouraev A.V., S.V. Semovski, M.N.Shimaraev, N.M. Mognard, B. Legresy, F. Remy. "Observations of lake Baikal ice from satellite altimetry and radiometry". Remote Sensing of Environment, 2007a, Vol. 108, issue 3, pp. 240-253

Kouraev A.V., S.V. Semovski, M.N.Shimaraev, N.M. Mognard, B. Legresy, F. Remy. "Ice regime of lake Baikal from historical and satellite data: Influence of thermal and dynamic factors". Limnology and Oceanography, 2007b, 52(3), 1268-1286.

Kouraev A.V., Zakharova E.A., Samain O., Mognard-Campbell N., Cazenave A. "Ob' river discharge from TOPEX/Poseidon satellite altimetry data", Remote Sensing of Environment, 93, 2004c, pp. 238-245

Kozhova, O.M., Izmest'eva, L.R. Eds. , 1998. Lake Baikal, Evolution and Biodiversity. Backhuys Publ., Leiden.

Krasnozhon, G. F. & Lyubomirova, K. S. 1987: Izucheniye ledovogo rezhima Severnogo Kaspiya po dannym meteorologicheskih sputnikov Zemli. (Study of ice cover in the northern Caspian from meteorological satellites.) Issle-dovaniye Zemli iz kosmosa (Study of Earth from Space) 5, 27–32. Moscow.

Laxon S., N. Peacock, and D. Smith, "High interannual variability of sea ice thickness in the Arctic region," Nature, 2003, vol. 425, no. 6961, pp. 947–950.

Lebedev, V. V. & P. L. Medres, 1966. Ledovyi rezhim Ladozhskogo ozera po materialam aviarazvedok. Sbornik rabot Leningradskoi GMO 3: 135–182. (Lake Ladoga ice covers condition by the aircraft surveys data. In Russian.)

Legrésy, B., & Rémy, F. (1997). Altimetric observations of surface characteris-tics of the Antarctic ice sheet. Journal of Glaciology, 43(144), 265-275.

Livingstone, D. (1999) Ice break-up on southern Lake Baikal and its relationship to local and regional air temperatures in Siberia and the North Atlantic Oscillation. Limnol Oceanogr 44, 1486–1497

Lobov A.L. Tsytsarin A.G., Perminov V.M. Formirovaniye poley osnovnyh gidrologo-gidrohimicheskih harakteristik v vodah Severnogo Kaspiya v ledoviy period (Formation of main hydrological and hydrochamical fields in the Northern Caspian during ice season. 1993. VINITY Deponent. 28.03.1993, N 2481-B93, 51 pp.

Mackay, A.W., Battarbee, R.W., Flower, R.J., Granin, N.G., Jewson, D.H., Ryves, D.B. & Sturm, M. (2003) Assessing the potential for developing internal diatom-based inference models in Lake Baikal. Limnology & Oceanography, 48, 1183-1192.

Mackay, A.W., Ryves, D.B., Battarbee, R.W., Flower, R.J., Jewson, D., Rioual, P. & Sturm, M. (2005). 1000 years of climate variability in central Asia: assessing the evidence using Lake Baikal diatom assemblages and the application of a diatom-inferred model of snow thickness. Global & Planetary Change, 46, 281-297.

Magnuson, J.J., Robertson D.M., Benson, B.J., Wynne, R.H., Livingstone, D.M., Arai, T., Assel, R.A., Barry, R.G., Card, V., Kuusisto, E., Granin, N.G., Prowse, T.D., Stewart, K.M., & Vuglinski, V.S. (2000). Historical Trends in Lake and River Ice Cover in the Northern Hemisphere. Science, Vol 289, Issue 5485, 1743-1746.

Maheu C., Cazenave A., Mechoso R. Water level fluctuations in the La Plata basin (South America) from Topex/Poseidon altimetry. Geophys. Res. Lett, 30,3,2003.

Marcus T. and D. J. Cavalieri, "Snow depth distribution over sea ice in the Southern Ocean from satellite passive microwave data," in Antarctic Sea Ice: Physical Processes, Interactions and Variability, M. O. Jeffries, Ed. Washington, DC: AGU, 1998, vol. 74, Antarctic Research Series, pp. 19–39.

Markus, T., & D.J. Cavalieri. (2000). An enhancement of the NASA Team sea ice algorithm. IEEE Trans. Geophys. Remote Sens., 38 (3), 1387-1398.

Medres, P. L., 1957. Ledovyi rezhim Ladozhskogo ozera po materialam aviarazvedok. Trudy GGI, Gidrometeoizdat, Leningrad, 66: 92–140. (Lake Ladoga ice cover conditions by the aircraft surveys data. In Russian.)

Mercier F., Cazenave A., Maheu C. Interannual lake level fluctuations in Africa from Topex/Poseidon: connections with ocean-atmosphere interactions over the Indian ocean. Global and Planet. Change, 32, 141-163, 2002

Mognard, N.M. and E.G. Josberger, Northern Great Plains 1996/97 seasonal evolution of snowpack parameters from satellite passive microwave measurements, Ann. Glaciol., 34, 15-23, 2002.

Papa F., B. Legresy, N. Mognard, E.G. Josberger, F. Remy. "Estimating terrestrial snow depth with the TOPEX/Poseidon altimeter and radiometer". IEEE Trans. Geosci. Remote Sens. 2002, 40, pp. 2162–2169.

Papa F., B. Legresy, N. Mognard, E. G. Josberger, and F. Remy, “Estimating terrestrial snow depth with the TOPEX/Poseidon altimeter and radiometer,” IEEE Trans. Geosci. Remote Sensing, vol. 40, pp. 2162–2169, Oct. 2002.

Pastukhov V.D. "Baikal's seal" /"Nerpa Baikala", Nauka, Novosibirsk, 1993, 271 pp

Ponchaut, F. and Cazenave, A. Continental lake level variations from TOPEX/POSEIDON (1993-1996). Earth and Planetary Sciences, 326, 13–20. 1998

Semovski, S.V., & Mogilev, N.Yu.. (2003). Ice and snow cover of Lake Baikal — application of satellite imagery in investigating their dynamics, Nordic Hydrology, 34, 33-50.

Semovski, S.V., Mogilev, N.Yu., & Sherstyankin, P.P. (2000). Lake Baikal ice: analysis of AVHRR imagery and simulation of under-ice phytoplankton bloom. Journal of Marine Systems, 27, 117-130.

Semovski, S.V., Mogilev, N.Yu., & Sherstyankin, P.P. (2000). Lake Baikal ice: analysis of AVHRR imagery and simulation of under-ice phytoplankton bloom. Journal of Marine Systems, 27, 117-130.

Sherstyankin, P.P. (1975) Experimental investigations of the lake Baikal under-ice light field, Moscow, Nauka, (in Russian).

Shimaraev, M.N., Domysheva, V.M., Sinyukovich, V.N., Kuimova, L.N., & Troitskaya, E.S. (2003). Manifestation of global climatic changes in Lake Baikal during the 20th century. In "Proceedings of the 7th Workshop on physical processes in natural waters 2-5 Yuly 2003. Petrozavodsk, Russia" (pp. 161-164). Petrozavodsk.

Shimaraev, M.N., Kuimova, L.N., Sinyukovich, V.N., & Tsekhanovskii, V.V. 2002b. Climate and hydrological processes in the basin of Lake Baikal in the XXth century. Meteorology and Hydrology, 3, 71-78, in Russian.

Spreen, G., L. Kaleschke, and G. Heygster Operational sea ice remote sensing with AMSR-E 89 GHZ Channels, IEEE International Geoscience and Remote Sensing Symposium Proceedings, IEEE 6, 4033-4036, 2005

Spreen, G., L. Kaleschke, and G. Heygster, Sea ice remote sensing using AMSR-E 89 GHz channels, J. Geophys. Res., 2008 doi:10.1029/2005JC003384

Steffen, K., Key, J., Cavalieri, D.J., Comiso, J., Gloersen, P., St.Germain, K., & Rubinstein, I. (1992). The estimation of Geophysical parameters using passive microwave algorithms. In Carsey F.D. (Ed), Microwave Remote Sensing of Sea Ice, AGU: Geophysical Monograph 68.

Stepanova V.A. Ledoviy rezhim Onezhskogo ozera i metody ego prognosa. (Ice regime of Lake Ladoga and methods for its forecast). Trudy GGI - Proceedings of the State Hydrological Institute, Leningrad, 1962, issue 80, pp. 66-125

Svendsen, E., Mätzler, C., & Grenfell, T. C. (1987). A model for retrieving total sea ice concentration from spaceborne dual-polarised passive microwave instrument operating near 90 GHz. Int. J. Remote Sensing, 8, 10, 1479-1487.

Swift, C. T. & Cavalieri, D. J. (1985). Passive microwave remote sensing for sea ice research. EOS. 66(49), 1210-1212

Terziev F.S., A. N. Kosarev, and A. A. Kerimov, Eds., Gidrometeorologiya i Gidrohimiya Morey (Hydrometeorology and Hydrochemistry of Seas). St.-Petersburg, Russia: Gidrometeoizdat, 1992, vol. VI, Caspian sea, Issue 1—Hydrometeorological Conditions.

The INTAS Project 99-1669 Team (2002). A new bathymetric map of Lake Baikal. Open-File Report on CD-ROM.

Todd, M.C., & Mackay, A.W. (2003). Large-Scale Climatic Controls on Lake Baikal Ice Cover. Journal of Climate Volume: Vol 16, 19, 3186-3199

Tsytsarin A., A. Skorokhod, L. Lissitsyna. 1999 Spatial Variability of Ionic Ratios Enclosed Sea Ice, Meteorology and Hydrology, N1, pp. 84-93 (in Russian).

Tsytsarin A.G., Gorelkin N.E., Nurbaev D.D. Aspekty zimnego gidrologicheskogo rezhima Aral'skogo morya i fiziko-himicheskiye svoystva l'da (Aspects of winter hydrological regime of the Aral sea and physical and chemical properties of ice. Moscow, 1993. 29 pp. VINITY Deponent. 22 Jan 1993, N 139-B93

Tsyzarin A.G. Solevoy i biogenniy sostav l'da i podlednoy vody Aral'skogo morya. (Salt and nutrients composition of the Aral sea ice and sub-ice water. Moscow, 1987. 24 pp. VINITY Deponent. 25 Dec 1987, N 9121-B87.

Ulaby, F.T., Moore, R.K. & Fung, A.K. (1986). Microwave remote sensing, Active and Passive, Vol. III, From theory to applications. Artech house, Inc.

Usachev, V. F., V. G. Prokacheva & V. V. Borodulin, 1985. Otsenka dinamiki ozernykh l'dov, snezhnogo pokrova i rechnykh razlivov distantsionnymi sredstvami. Gidrometeoizdat, Leningrad. 103 pp. (The lake ice dynamics, snow covering and river floods estimation by remote sensing. In Russian.)

Verbolov, V. I., Sokol'nikov, V. M., & Shimaraev, M. N. (1965). Hydrometeorological regime and heat balance of the Lake Baikal. Moscow-Leningrad: “Nauka...publishers 373 pp. (In Russian).

Wüest, A, Ravens, T.M., Granin, N.G., Kocsis, O., Schurter, M., & Sturm, M. (2005). Cold intrusions in Lake Baikal: Direct observational evidence for deep-water renewal. Limnol. Oceanogr, 50(1), 184–196.

Zakharova E.A., Kouraev A.V., Cazenave A, Seyler F. "Amazon river discharge estimated from Topex/Poseidon satellite water level measurements", Comptes Rendus - Geoscience, 2006, Vol 338, No 3, 188-196.